Journal of Chromatography A, 1217 (2010) 8212–8221

Contents lists available at ScienceDirect

Journal of Chromatography A

journal homepage: www.elsevier.com/locate/chroma

Hypercrosslinking: New approach to porous polymer monolithic capillary columns with large surface area for the highly efficient separation of small molecules

Jiri Urban[a], Frantisek Svec[b], Jean M.J. Fréchet[a,b,*]

[a] Department of Chemistry, University of California, Berkeley, CA 94720, USA
[b] The Molecular Foundry, E.O. Lawrence Berkeley National Laboratory, Berkeley, CA 94720, USA

ARTICLE INFO

Article history:
Received 13 September 2010
Received in revised form 22 October 2010
Accepted 25 October 2010
Available online 31 October 2010

Keywords:
Hypercrosslinked polymer monolith
Poly(styrene-*co*-vinylbenzyl chloride-*co*-divinylbenzene)
Reversed phase chromatography
Size-exclusion chromatography
Small molecules

ABSTRACT

Monolithic polymers with an unprecedented surface area of over 600 m^2/g have been prepared from a poly(styrene-*co*-vinylbenzyl chloride-*co*-divinylbenzene) precursor monolith that was swollen in 1,2-dichloroethane and hypercrosslinked via Friedel-Crafts reaction catalyzed by ferric chloride. Both the composition of the reaction mixture used for the preparation of the precursor monolith and the conditions of the hypercrosslinking reaction have been varied using mathematical design of experiments and the optimized system validated. Hypercrosslinked monolithic capillary columns contain an array of small pores that make the column ideally suited for the high efficiency isocratic separations of small molecules such as uracil and alkylbenzenes with column efficiencies reproducibly exceeding 80,000 plates/m for retained compounds. The separation process could be accelerated while also improving peak shape through the use of higher temperatures and a ternary mobile phase consisting of acetonitrile, tetrahydrofuran, and water. As a result, seven compounds were well separated in less than 2 min. These columns also facilitate separations of peptide mixtures such as a tryptic digest of cytochrome c using a gradient elution mode which affords a sequence coverage of 93%. A 65 cm long hypercrosslinked capillary column used in size exclusion mode with tetrahydrofuran as the mobile phase afforded almost baseline separation of toluene and five polystyrene standards.

1. Introduction

Monolithic columns with excellent permeability to flow emerged in the early 1990s and enabled rapid chromatographic separations at high flow velocities [1–4]. Theoretical models developed later by Liapis, Guiochon, Desmet, and others assigned their enhanced performance to low resistance to mass transfer enabled by morphological features of their internal structure [5–9]. Detailed overview of the characteristics and applications of polymer-based monolith is presented in many review articles [10–22]. Typical monolithic columns prepared from porous polymers [3] comprise aggregated nonporous microglobules and exhibit modest surface areas in the range of tens of m^2/g. Since these monolithic columns completely lack mesopores, they are almost ideally suited for the fast separation of molecules such as proteins [23], nucleic acids [24], and synthetic polymers [25] using the gradient elution mode. While the small surface area of current polymer monoliths provides distinct advantages in the separations of large molecules for which diffusional mass transport is slow, it does not provide the desirable high number of interaction sites required for the separation of small molecules in isocratic mode. For example, in our early experiments, we found that monolithic poly(styrene-*co*-divinylbenzene) column separated alkylbenzenes with an efficiency of only 18,000 plates/m [26]. Several recent attempts to optimize the porous properties of methacrylate polymer monoliths have led to columns affording 35,000–50,000 plates/m for benzene as the retained analyte [27–31]. In addition, several new approaches have also been explored including the polymerization of a crosslinking monomer [32–35], the termination of the polymerization reaction at an early stage [36–38], and the use of polymerization at high temperatures [39–41]. In spite of all of these efforts, it has always proven difficult to prepare polymer monoliths possessing both large through pores and a multiplicity of small pores in a single step and alternative approaches to do so are highly desirable.

Several decades ago, Davankov prepared large surface area materials from preformed polymer precursors in a technique termed "hypercrosslinking" [42–45]. The original implementation involved linear polystyrene crosslinked via a Friedel-Crafts alkylation with bis-electrophiles to afford materials containing mostly

* Corresponding author at: Department of Chemistry, University of California, Berkeley, CA 94720, USA. Tel.: +1 510 643 3077; fax: +1 510 643 3079.
E-mail address: frechet1@gmail.com (J.M.J. Fréchet).

0021-9673/$ – see front matter © 2010 Elsevier B.V. All rights reserved.
doi:10.1016/j.chroma.2010.10.100

small pores [42,46]. Davankov later extended hypercrosslinking to previously crosslinked polystyrene copolymers [44]. Other groups carried out hypercrosslinking using porous poly(vinylbenzyl chloride-*co*-styrene-*co*-divinylbenzene) resins [47–50]. For example, Sherrington and coworkers have prepared polymer beads with a bimodal pore size distribution and surface areas as high as 1055 m^2/g [48]. Similarly, we hypercrosslinked macroporous poly(vinylbenzyl chloride-*co*-divinylbenzene) to obtain beads with a surface area exceeding 2000 m^2/g [51,52]. Small diameter hypercrosslinked beds have also been used as stationary phase in HPLC [53–55].

Recently, we have demonstrated for first time the preparation of hypercrosslinked porous polymer monoliths exhibiting a large surface area and their use in capillary columns for the fast and efficient separation of small molecules as well as for rapid size-exclusion chromatography [56].

In this report we focus on the optimization of reaction conditions for the preparation of highly performing hypercrosslinked monolithic capillary columns. We also explore the factors that affect the formation of network of small pores within the monolith for enhanced column efficiencies.

2. Experimental part

2.1. Materials

Styrene (99%), vinylbenzyl chloride (mixture of 3- and 4-isomers, 97%), divinylbenzene (80%, technical grade), 2,2′-azobisisobutyronitrile (98%), acetonitrile (HPLC grade), uracil, benzene, ethylbenzene, amylbenzene, ribonuclease A, cytochrome c, myoglobin, α-chymotrypsinogen A and albumin were all obtained from Sigma–Aldrich (St. Louis, MO, USA). Propylbenzene and butylbenzene were purchased from Matheson Coleman & Bell (Los Angeles, CA, USA), toluene from EMD Chemicals (Gibbstown, NJ, USA). The monomers styrene, vinylbenzyl chloride, and divinylbenzene were purified by passage through a bed of basic alumina to remove the inhibitors. Ferric chloride was purchased from Fisher (New Jersey, NJ, USA). Polystyrene standards with molar masses ranging from 580 to 1,870,000 were obtained from Viscotek (Houston, TX, USA). Polyimide-coated 100 μm I.D. fused silica capillaries were purchased from Polymicro Technologies (Phoenix, AZ, USA).

2.2. Preparation of capillary columns

The fused-silica capillaries were rinsed with acetone, water, 200 mmol/L sodium hydroxide, water, 200 mmol/L HCl, and ethanol. Then, a 20% (v/v) solution of 3-(trimethoxysilyl)propyl methacrylate in ethanol with an apparent pH value of 5 adjusted using acetic acid, was pumped through the capillary for 1 h using a syringe pump. After this vinylization procedure, the capillaries were rinsed with ethanol, and dried with a stream of nitrogen.

Generic monoliths were prepared in capillaries using *in situ* polymerization of mixtures of styrene, vinylbenzyl chloride, and divinylbenzene dissolved in binary porogen solvent containing toluene and 1-dodecanol. 2,2′-Azobisisobutyronitrile (AIBN) (1%, w/w, with respect to monomers) was used as the initiator. The polymerization mixtures were purged with nitrogen for 10 min and filled in the vinylized capillaries using a syringe. Both ends of the capillary were sealed with rubber stoppers and the capillary was placed in a water bath. Polymerization was carried out at 70 °C for 20 h. Both ends of the capillary were then cut to adjust its lengths and the monolithic column was washed with acetonitrile. Simultaneously, excess of the polymerization mixture was polymerized in a glass vial under the same conditions. The vial containing the monolith formed from the bulk polymerization mixture was carefully crushed, the polymer cut into small pieces, Soxhlet extracted with methanol for 12 h to remove any soluble compounds, and vacuum dried at 60 °C overnight. This polymer was used for the porosimetric measurements.

2.3. Hypercrosslinking

The hypercrosslinking reaction in batch was carried out using 1.70 g monolithic material pre-swollen in 20 mL of 1,2-dichloroethane for 2 h. The Lewis acid catalyst $FeCl_3$ (1 g) was then added to the slurry cooled in an ice bath. Once the catalyst was homogeneously dispersed, the mixture was allowed to come to the room temperature. The hypercrosslinking reaction was then allowed to proceed at 80 °C for 24 h, unless mentioned otherwise. The resulting polymer was separated and washed with methanol, then 0.5 mol/L HCl in acetone, and then again with methanol followed by drying *in vacuo*. Hypercrosslinking of monoliths in capillary columns followed a similar procedure. The columns were flushed with 1,2-dichloroethane at a flow rate of 0.25 μL/min for 2 h. The filtered solution of 1 g of $FeCl_3$ in 20 mL of 1,2-dichloroethane was pumped through the columns at a flow rate of 0.25 μL/min for 2 h and the columns were held in an ice bath for 1 h. Unless otherwise mentioned, the reaction was carried out at 80 °C for 2 h. The hypercrosslinking columns were then washed with water overnight and tested.

2.4. Instrumentation

A Dionex Ultimate 3000 HPLC system (Sunnyvale, CA, USA) equipped with a 3-nL UV detection cell and an external micro-valve injector with a 4-nL inner sampling loop (Valco, Houston, USA) was used for the chromatographic experiments. Typically, isocratic reversed-phase chromatography was carried out using a mixture of 80% acetonitrile and 20% water as the mobile phase. Solutions of 0.1% formic acid in acetonitrile and water, respectively, were used as the mobile phases for elution in the gradient mode. Tetrahydrofuran at a flow rate of 0.5 μL/min and polystyrene standards were used for size-exclusion chromatography.

Nitrogen adsorption/desorption isotherms were measured using a Micromeritics ASAP 2010 surface area and porosimetry analyzer (Norcross, GA) and used for the calculation of surface areas.

2.5. Separation of tryptic digest

Cytochrome c (2.5 mg/mL) was diluted with a 100 mmol/L ammonium bicarbonate solution, trypsin added at a substrate-to-enzyme ratio of 50:1 (w/w) and the solution was incubated at 37 °C for 20 h. The proteolysis was terminated by lowering the pH via addition of formic acid to the solution. Chromatographic experiments with mass spectrometric (MS) detection were performed using a liquid chromatography system consisting of an Agilent 1200 Series capillary pump and external Valco injector with 4 nL injection loop. Linear gradient of 5–40% acetonitrile with 0.1% formic acid in 0.1% aqueous formic acid was used at a flow rate of 0.5 μL/min. MS detection was carried out using a micrOTOF-Q (Bruker Daltonics, Fremont, CA, USA) equipped with nanospray interface in positive ion mode with a m/z range of 400–1500.

2.6. Chromatographic characterization

The effect of linear velocity of the mobile phase, u, on efficiency of hypercrosslinked monolithic capillary columns defined as height equivalent to theoretical plate, HETP, was determined from plots described by van Deemter equation [57].

The flow resistance of the columns is characterized by the column permeability, K_F, that is calculated using the Darcy's equation [58]:

$$K_F = \frac{F_m \eta L}{\Delta p \pi r^2} \quad (1)$$

where F_m is the flow rate, η is the mobile-phase viscosity, Δp is the pressure drop across the column, and r is the column inner radius. The total porosity, ε_T, was determined using equation:

$$\varepsilon_T = \frac{V_M}{V_C} \quad (2)$$

where V_M is the elution volume of the non-retained uracil and V_C is the overall volume of the empty cylindrical column. The inner or mesopore porosity, ε_i, defined as

$$\varepsilon_i = \frac{V_M - V_0}{V_C} \quad (3)$$

was determined from the results of inverse size-exclusion chromatography and calculated as the difference of the elution volume of uracil that permeates all pores and elution volume V_0 of the polystyrene standard with a molar mass of 1,870,000 which was assumed to be totally excluded from the mesopores. This difference is normalized by the empty column volume. Extra column volume of 0.24 μL was subtracted from both elution volumes.

2.7. Design of experiments

The experimental region of composition of the polymerization mixture is irregular. Hence, we applied the D-optimal design using a home-written routine in MATLAB (MathWorks, Natick, MA, USA). Five variables included in the experimental design were the percentages of styrene (ST), vinylbenzyl chloride (VBC), divinylbenzene (DVB), toluene (TOL) and 1-dodecanol (DOD). The sum of the volume fractions of all these components in the polymerization mixture equaled 100%. As AIBN was the only component for which concentration was kept constant in the preparation of monolithic columns, the compositions of the polymerization mixtures do not include AIBN. The concentration limits of the polymerization mixture space were adjusted using subsequent mixture designs in three steps with gradually narrowing concentration ranges of the five components. The final design range for the mixture covered space defined within 10–24% ST, 4–23% VBC, 7–24% DVB, 7–21% TOL, and 38–55% DOD. The HETP for benzene at a linear flow velocity of 0.5 mm/s ($HETP_{BE}$) and mesopore porosity ε_i were used as the response factors. Another home-written routine in MATLAB was used for the non-linear evaluation of multivariate data. By removing insignificant variables, a model describing the effects of the experimental parameters on the efficiency and mesopore porosity of hypercrosslinked capillary columns was improved and its predictive power increased. The number of parameters used in the initial model was gradually reduced, depending on the value of the calculated probability factors f, which is a measure of the relevance of the experimental variables on the response. Probability factors higher than 0.05 mean that the parameter does not affect significantly the system response. The terms related to these parameters are then removed from the model in several subsequent steps. Only a single parameter with the highest calculated f value is removed in each step.

3. Results and discussion

3.1. Preparation of hypercrosslinked monoliths

In contrast to general perception, even highly crosslinked copolymers of styrene, vinylbenzyl chloride, and divinylbenzene may swell in thermodynamically good solvents. Due to its higher reactivity, the divinylic crosslinker polymerizes faster [59] thus becoming more rapidly depleted from the polymerization mixture than its monovinyl counterparts. As the polymerization reaction approaches completion, the chains created from the remaining mixture poor in crosslinking monomer are sparsely crosslinked and form a swellable layer. Jerabek suggested the existence presence of such layers based on inverse size-exclusion chromatography data [60,61]. These layers containing chloromethyl groups are amenable to hypercrosslinking via Friedel-Crafts alkylation. To carry out this reaction, the monolith is filled with a solvent that swells the surface layer followed by addition of the catalyst, which initiates the hypercrosslinking process immobilizing the polymer chains in their solvated state and forming small pores that persist even after removal of the solvent. It is the creation of these new pores that leads to a high surface area monolith better suited for the separation of small molecules.

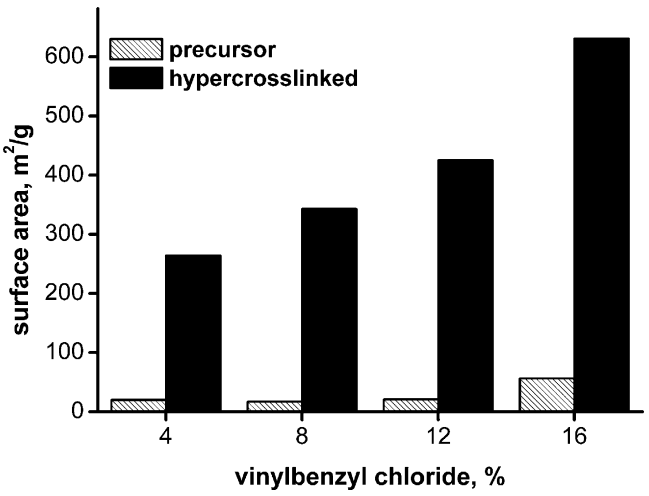

Fig. 1. Effect of hypercrosslinking of poly(styrene-*co*-vinylbenzyl chloride-*co*-divinylbenzene) precursor monolith on the specific surface area. Conditions: polymerization mixture used for the preparation of precursor monolith: 16% styrene + vinylbenzyl chloride, 24% divinylbenzene, 18% toluene, 42% 1-dodecanol, 1% (with respect to monomers) AIBN; hypercrosslinking 24 h at 80 °C.

As might be expected, the extent of hypercrosslinking depends on the percentage of divinylbenzene in the monomer mixture and the ratio of functional vinylbenzyl chloride and inert styrene [56]. In our current study, we first varied the percentages of monovinyl monomers styrene and vinylbenzyl chloride in the polymerization mixture while keeping constant the percentages of divinylbenzene, toluene, and 1-dodecanol at 24, 18, and 42%, respectively. Fig. 1 shows that while the precursor monoliths only exhibited a specific surface area of 17–56 m^2/g, the hypercrosslinked monoliths had surface areas of up to 631 m^2/g. This value compares favorably to other polymer-based monoliths [37,62–65] and even significantly exceeds the surface area of 300 m^2/g measured for the silica monoliths developed by Tanaka [4,66].

The porous properties of bulk monoliths prepared in glass vials shown in Fig. 1 were measured using nitrogen adsorption/desorption in the dry state. While these surface areas are a good indication of the presence of mesopores, pore volumes calculated from these data are less realistic since they do not represent the large through pores. In addition, the monoliths prepared within capillary columns operate in a solvating mobile phase, which may also change the porous properties of the monoliths [67]. In contrast, chromatographic methods enable the monitoring of the elution volume of a small unretained probe molecule such as uracil or toluene, which affords a value of the total pore volume present in the col-

Table 1
Effect of hypercrosslinking time on surface area and column efficiency for uracil $HETP_{UR}$. Conditions: monolith prepared from polymerization mixture containing 12% styrene, 12% vinylbenzyl chloride, 16% divinylbenzene, 18% toluene, 42% 1-dodecanol. Hypercrosslinking: swelling in dichloroethane for 2 h followed by addition of $FeCl_3$, and reacted at a temperature of 80 °C. $HETP_{UR}$ determined at a linear velocity of 0.5 mm/s.

	Hypercrosslinking time, h					
	0	0.5	1	2	18	24
Surface area, m^2/g	21	222	283	408	418	424
$HETP_{UR}$, μm	34.8	27.5	23.7	15.5	15.5	16.1

umn. Therefore, this technique was used in all of our subsequent experiments.

The extent of hypercrosslinking is also affected by reaction time and the results presented in Table 1 demonstrate that a rapid increase in surface area occurs during the first two hours. Extending the reaction time beyond 2 h does not lead to any appreciable further increase in surface area. This finding correlates well with the results of Ahn et al. [48] who also noticed a rapid increase in surface area only during the first 2 h of the hypercrosslinking reaction of porous beads of poly(vinylbenzyl chloride-*co*-styrene-*co*-divinylbenzene). This was attributed to the two-step reaction mechanism involving first the generation of an "internal" electrophile followed by intramolecular formation of dihydroanthracene structures. The column efficiencies also shown in Table 1 follow the same path as the surface area reaching their maximum after 2 h with no further change observed for longer reaction times.

In order to better describe the overall effect of the polymerization mixture used for the preparation of the precursor monolithic columns on column efficiency, porosity, permeability, and mass transport resistance, we systematically changed the composition using the mixture-design approach. The composition space was adjusted in three steps using subsequent mixture designs with gradually narrowing concentration ranges of all five components.

Table 2 confirms the strong correlation between the composition of the polymerization mixture and the porous as well as hydrodynamic properties of hypercrosslinked monolithic columns. Total porosity, ε_T, correlates well with the volume percentage of porogens in the polymerization mixture. Hypercrosslinking should not lead to any appreciable change in total porosity since the reaction does not add any significant mass to the original polymer, which would then decrease the pore volume [56]. In contrast, column permeability, K_F, decreases with increasing mesopore content in the monolithic bed, ε_i. The mesoporous polymer layer created from expanded polymer chains occupies some space in the large through pores and decreases their size. The larger the volume of the newly created mesoporous polymer layer, the lower the column permeability. Importantly, the larger volume of the mesoporous polymer layer also affords a larger surface area available for interactions during the chromatographic separation, which results in better column efficiency expressed as HETP. The efficiency also correlates well with resistance to the mass transfer. The most efficient columns feature the lowest values of the *C* coefficient in the van Deemter equation.

3.2. Repeatability of hypercrosslinking

While we have already demonstrated excellent repeatability of porous polymer monolithic columns [68], hypercrosslinking adds a new step and both column-to-column and run-to-run repeatability need to be revisited. Three separate batches of three hypercrosslinked columns were prepared at different days using polymerization mixture of column 15 (Table 2). Column efficiency was determined for all nine hypercrosslinked monolithic capillary columns using uracil and benzene at different flow rates. The van Deemter plots coincided well as evidenced by relative standard deviation (RSD) values of 2.3 and 1.5% for uracil and benzene, respectively. The average RSD for retention times in ten runs using three different columns were 2.7 for both uracil and benzene, and 2.6 for ethylbenzene.

3.3. Design of experiments to improve efficiency

The results collected in Table 2 do not allow the direct evaluation of the effects of the individual experimental factors, i.e. percentages of the individual components in the polymerization mixture, on the efficiency and mesopore porosity of hypercrosslinked monoliths and a multiparameter statistical analysis must be used. We applied a D-optimal design of mixtures for all 17 hypercrosslinked monolithic columns we prepared with defined efficiency and mesopore porosity shown in Table 2. We deleted all constant and quadratic terms from the general second-order polynomial model to obtain

Table 2
Effect of composition of the polymerization mixture on characteristics of hypercrosslinked monolithic capillary columns.

Column	ST, %	VBC, %	DVB, %	TOL, %	DOD, %	ε_T, %	ε_i, %	K_F, m^2	$HETP_{BE}$, μm	C_{BE}, 10^{-3} s
1	11.7	13.7	16.5	8.9	49.1	57.8	15.8	1.4E−14	595	934.0
2	14.8	14.9	11.1	20.7	38.5	58.8	16.4	7.3E−15	170	118.3
3	11.0	22.6	9.1	8.9	48.4	55.1	13.3	2.4E−14	371	523.8
4	13.0	12.8	9.8	10.0	54.4	59.0	14.6	1.6E−14	363	596.6
5	9.8	22.2	15.2	8.4	44.3	52.1	10.5	1.9E−14	763	1036.2
6	19.6	19.9	7.7	7.6	45.3	51.4	17.3	1.3E−14	637	1138.0
7	16.2	16.7	16.2	11.0	39.9	55.7	24.1	4.3E−15	198	98.1
8	11.9	12.0	17.2	17.0	41.9	54.6	14.4	9.9E−15	144	133.5
9	17.1	12.2	17.3	12.0	41.4	49.6	18.2	4.1E−15	82	42.1
10	17.0	12.6	11.8	16.8	41.7	54.0	12.6	7.9E−15	297	389.3
11	17.7	18.3	9.1	9.0	45.9	52.3	16.2	5.6E−15	278	341.7
12	10.1	19.2	10.1	10.2	50.4	58.1	12.8	9.5E−15	322	441.0
13	19.8	10.1	10.0	19.7	40.5	57.8	16.8	8.4E−15	54	50.8
14	12.0	4.2	23.4	17.5	42.8	57.3	22.5	3.2E−15	83	24.2
15	12.1	12.1	16.0	18.0	41.8	59.4	22.8	1.6E−15	38	22.5
16	18.1	6.0	16.2	17.9	41.9	60.1	21.2	4.6E−16	48	26.0
17	23.7	8.4	7.9	18.3	41.6	59.7	16.2	1.1E−14	49	13.5

$\varepsilon_T = V_M/V_C$, where V_M is the elution volume of uracil and V_C is the geometrical volume of the empty cylindrical column.
$\varepsilon_i = (V_M - V_0)/V_C$, where V_0 is the elution volume of polystyrene standard with M = 1,870,000.
K_F – column permeability calculated using Eq. (1).
$HETP_{BE}$ – height equivalent to theoretical plate for benzene at a linear velocity of 0.5 mm/s.
C – mass transport kinetics parameter from C-term of van Deemter equation.

Table 3
The optimization of the original model of Eq. (4) for column efficiency in reversed phase mode RP and mesopore porosity calculated from inverse size-exclusion chromatography, ISEC using the probability factors *f*.

RP	*f*								
	Step 1	Step 2	Step 3	Step 4	Step 5	Step 6	Step 7	Step 8	Step 9
x_1	0.6834	0.6133	0.5264	0.5357	0.5668	0.5718	–	–	–
x_2	0.3381	0.2159	0.1455	0.0679	0.0404	0.0113	0.0081	0.0018	0.0010
x_3	0.4430	0.1883	0.1224	0.0883	0.0723	0.0342	0.0125	0.0009	0.0006
x_4	0.8443	0.8250	0.7127	–	–	–	–	–	–
x_5	0.8943	0.9263	–	–	–	–	–	–	–
x_1x_2	0.7220	0.6212	0.5645	0.5656	0.7398	–	–	–	–
x_1x_3	0.7386	0.5549	0.4726	0.4685	0.4160	0.3921	0.4277	–	–
x_1x_4	0.8935	0.5709	0.4949	0.4482	0.4843	0.3409	0.2852	0.4351	–
x_1x_5	0.6850	0.6152	0.4886	0.5019	0.4795	0.4716	0.2379	0.2974	0.0455
x_2x_3	0.8578	0.6555	0.5595	0.6016	–	–	–	–	–
x_2x_4	0.7935	0.3228	0.1884	0.1241	0.0556	0.0372	0.0285	0.0147	0.0142
x_2x_5	0.3310	0.2182	0.1470	0.0626	0.0392	0.0119	0.0085	0.0026	0.0013
x_3x_4	0.9113	–	–	–	–	–	–	–	–
x_3x_5	0.3210	0.1709	0.0990	0.0638	0.0497	0.0231	0.0056	0.0008	0.0006
x_4x_5	0.7895	0.6027	0.4595	0.2800	0.2219	0.1318	0.0981	0.0736	0.0432
R	0.9280	0.9275	0.9272	0.9244	0.9197	0.9181	0.9139	0.9064	0.8995

SEC	*f*										
	Step 1	Step 2	Step 3	Step 4	Step 5	Step 6	Step 7	Step 8	Step 9	Step 10	Step 11
x_1	0.686	0.617	0.427	0.382	0.478	0.231	0.016	0.026	0.003	0.001	0.000
x_2	0.636	0.666	0.907	–	–	–	–	–	–	–	–
x_3	0.473	0.375	0.368	0.351	0.495	0.586	–	–	–	–	–
x_4	0.506	0.329	0.174	0.149	0.100	0.101	0.015	0.022	0.031	0.001	0.000
x_5	0.293	0.243	0.218	0.054	0.060	0.055	0.056	0.095	0.400	0.698	–
x_1x_2	0.473	0.373	0.258	0.232	0.294	0.184	0.013	0.015	0.047	0.002	0.002
x_1x_3	0.795	–	–	–	–	–	–	–	–	–	–
x_1x_4	0.731	0.530	0.261	0.239	0.351	0.246	0.004	0.005	0.011	0.007	0.000
x_1x_5	0.608	0.595	0.519	0.412	0.491	0.240	0.063	0.121	–	–	–
x_2x_3	0.464	0.362	0.348	0.329	0.274	0.243	0.273	–	–	–	–
x_2x_4	0.702	0.543	0.461	0.434	–	–	–	–	–	–	–
x_2x_5	0.640	0.676	–	–	–	–	–	–	–	–	–
x_3x_4	0.532	0.532	0.394	0.365	0.635	–	–	–	–	–	–
x_3x_5	0.370	0.276	0.262	0.241	0.349	0.339	0.118	0.095	0.446	–	–
x_4x_5	0.143	0.102	0.085	0.071	0.089	0.088	0.055	0.102	0.117	0.078	0.004
R	0.7666	0.7647	0.7603	0.7600	0.7469	0.7423	0.7366	0.7138	0.6657	0.6538	0.6508

x_1–x_5 are percentages of individual compounds in the polymerization mixture (x_1 – styrene, x_2 – chloromethylstyrene, x_3 – divinylbenzene, x_4 – toluene, x_5 – 1-dodecanol); *R* is correlation coefficient.

Eq. (4). This equation correlates the effects of five experimental factors x_1 through x_5 representing percentages of ST, VBC, DVB, TOL, and DOD in the polymerization mixture, respectively, with response y on plate height for benzene $HETP_{BE}$ and mesopore porosity ε_i:

$$y = p_1x_1 + p_2x_2 + p_3x_3 + p_4x_4 + p_5x_5 + p_6x_1x_2 + p_7x_1x_3 + p_8x_1x_4 + p_9x_1x_5 + p_{10}x_2x_3 + p_{11}x_2x_4 + p_{12}x_2x_5 + p_{13}x_3x_4 + p_{14}x_3x_5 + p_{15}x_4x_5 \quad (4)$$

Parameters p_1–p_5 represent the extent of effect of these individual components. The cross-term interaction parameters p_6–p_{15} account for combined effects of the components in the polymerization mixture. The parameters may be either synergistic (increasing response) or antagonistic (decreasing response). The significance of the effects of the parameters p_1–p_{15} in Eq. (4) on column efficiency and mesopore porosity was judged in several subsequent steps as illustrated in Table 3. The experimental factors were removed in steps based on the probability factors f_i, which are a measure of the effect of experimental factors on the response. Values of probability factors larger than 0.05 mean that the parameter does not affect significantly the response at a probability level of 95%, hence the terms with these parameters were removed from the model. Only a single parameter with the highest *f* value was removed in each step [69,70].

After cancelling the insignificant cross-term factors, we obtained the optimized models for column efficiency and mesopore (inner) porosity as a function of composition of the polymerization mixture. Experimental factors with high absolute values of the regression parameter p_i affect the targeted properties most significantly. Factors p_i for both original non-simplified and optimized model are listed in Table 4. The test of accuracy of our model for column efficiency revealed that a deviation between predicted and experimental value exceeded 100 μm for only three columns out of 17 while the average absolute deviation was 40 μm. The accuracy for mesopore porosity was even better since only three columns exhibited absolute deviation higher than 4% and the average value was 1.7%. The linear correlation confirms the good match of the predicted and measured values with correlation coefficients *R* of 0.95 and 0.80 for column efficiency and mesopore porosity, respectively.

Table 4 clearly shows that two main factors affect the column efficiency: synergistic percentage of the vinylbenzyl chloride (x_2) and antagonistic percentage of crosslinker divinylbenzene (x_3). This means that HETP increases at a higher concentration of vinylbenzyl chloride in the polymerization mixture, which equals reduction in the column efficiency. In contrast, a higher concentration of divinylbenzene affords columns with higher efficiency. It is also apparent that porogenic solvents alone contribute little to the column efficiency. As anticipated, these results confirm that the extent of hypercrosslinking depends on the percentage of divinylbenzene in the monomer mixture, which controls the number and length of

Table 4
Regression coefficients p_1–p_{15} for non-optimized (A) and optimized (B) models of column efficiency in reversed phase mode RP and mesopore porosity calculated from inverse size-exclusion chromatography, ISEC.

	p_1	p_2	p_3	p_4	p_5	p_6	p_7	p_8	p_9	p_{10}	p_{11}	p_{12}	p_{13}	p_{14}	p_{15}
RP															
(A)	353.0	781.0	−802.0	−183.0	36.0	−4.0	2.3	−4.6	−7.5	−1.8	−5.4	−15	4.8	15.1	4.8
(B)	–	386.0	−366.0	–	–	–	–	–	−0.5	–	−4.9	−7.1	–	8.1	1.1
ISEC															
(A)	3.75	2.59	9.13	7.20	1.89	−0.09	−0.04	−0.13	−0.07	−0.15	−0.06	−0.05	−0.15	−0.17	−0.15
(B)	2.32	–	–	2.99	–	−0.05	–	−0.12	–	–	–	–	–	–	−0.04

Table 5
Composition of the polymerization mixtures and efficiency $HETP_{BE,calc}$ of hypercrosslinked monolithic columns for benzene calculated according to the optimized model for column efficiency shown in Table 4 and comparison values measured for the prepared column. Conditions: mobile phase acetonitrile–water (80:20), linear flow velocity 0.5 mm/s.

Column	ST, %	VBC, %	DVB, %	TOL, %	DOD, %	$HETP_{BE,calc}$, μm	$HETP_{BE,exper}$, μm	Δ, μm[a]
C1	16.8	8.2	15.0	18.8	41.3	20	46	26
C2	20.7	7.2	12.3	18.9	40.9	11	39	28

[a] Δ Absolute deviation between the predicted and experimental value.

hypercrosslinkable loose chains, and the ratio of functional vinylbenzyl chloride and inert styrene that affects the frequency of reactive sites along the loose chains.

Table 4 also shows that mesopore porosity is mostly controlled by two different synergistic factors: percentage of styrene (x_1) and toluene (x_4). Three other parameters are antagonistic but their effect is much smaller. The difference in the factors affecting the column efficiency and mesopore porosity can result from different degree of solvation of the hypercrosslinked layer in aqueous acetonitrile and tetrahydrofuran mobile phase used for the measurements of efficiency and mesopore porosity.

The optimized model described above was developed to enable the preparation of columns with the desired predetermined efficiency. Using this model for column efficiency we calculated two polymerization mixtures to obtain $HETP_{BE}$ equal to 20 and 11 μm while keeping the percentage of all monomers at 40%. Interestingly, the percentages of toluene and 1-dodecanol varied within a narrow window of 18–20% and 41–42%, respectively. Table 5 shows the polymerization mixtures used and the difference between the set and actual values of the column efficiency. Although the results confirm the validity of our model, the differences between the predicted and experimental efficiency are 20 and 11 μm. These values remain within the deviation range of 40 μm found during optimization of the model but are rather large. This finding indicates that the prediction power of the model is reduced in the range of low values of HETP and thus, another variable needs to be taken into consideration to achieve a better match between prediction and experiment.

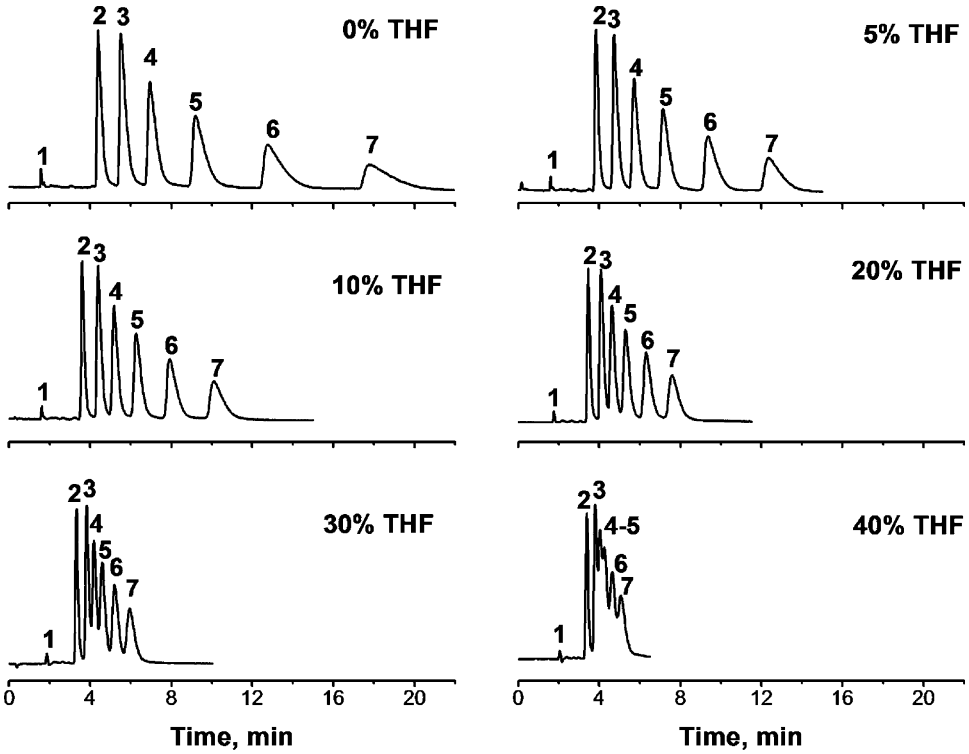

Fig. 2. Effect of percentage of tetrahydrofuran in the mobile phase on the separation of small molecules. Conditions: precursor column (C2, Table 5) 100 μm × 130 mm; hypercrosslinked for 2 h at 90 °C; ternary mobile phase 20% water, 80% THF + ACN, flow rate 0.5 μL/min. UV detection at 254 nm; column temperature 20 °C. Analytes: uracil (1), benzene (2), toluene (3), ethylbenzene (4), propylbenzene (5), butylbenzene (6), and pentylbenzene (7).

Table 6
Peak asymmetry for pentylbenzene AS_{PB} and resolution for peak pairs benzene–toluene $R_{BE,TO}$ and toluene–ethylbenzene $R_{TO,EB}$ at various percentages of tetrahydrofuran in the mobile phase containing acetonitrile and 20% water.

	Tetrahydrofuran, %					
	0	5	10	20	30	40
AS_{PB}	3.88	2.55	2.10	1.66	1.59	–
$R_{BE,TO}$	2.33	2.38	2.28	2.04	1.87	–
$R_{TO,EB}$	2.25	2.00	1.79	1.39	1.06	–

3.4. Temperature of hypercrosslinking

In contrast to the previous mapping of the experimental space available for the preparation of the precursor monolith, we focused on the next step, hypercrosslinking with two variables: reaction time and temperature. While, as mentioned earlier, a reaction time of 2 h was found to afford a monolith with the largest surface area, reaction temperature is also significant. Using precursor column C2 from Table 5 hypercrosslinking at 80 °C affords a column with $HETP_{BE}$ of 39 μm. An increase in temperature to 90 °C results in a column with a significantly lower $HETP_{BE}$ of 29 μm, a value that is much closer to the predetermined target. However, further increases in temperature do not lead to any improvement in column efficiency.

3.5. Effect of mobile phase

The typical mobile phase used for the separation of small hydrophobic molecules in the isocratic reversed phase mode is a mixture of water and acetonitrile. Fig. 2a shows the elution profile of alkylbenzenes using 20% aqueous acetonitrile. All compounds are baseline separated but a significant tailing is observed for the longer retained peaks. This tailing can be attributed to the diffusional mass transport in micropores present in the hypercrosslinked monolithic stationary phase. A similar problem noticed a long time ago for particulate porous separation media prepared from styrene and divinylbenzene was partly solved by using a ternary mixture comprising water and both thermodynamically poor and good solvents for the polymer [71,72]. This approach led to a significantly improved peak shape and was attributed to the partial swelling of the polymer that fills and thus "closes" the micropores.

Fig. 2 shows the effect of addition of tetrahydrofuran to the aqueous acetonitrile mobile phase on peak shape and resolution of alkylbenzenes in hypercrosslinked monolithic columns. The asymmetry factors for amylbenzene presented in Table 6 decrease from the original value of 3.9 to 1.6 in the ternary mobile phase containing 30% tetrahydrofuran. Addition of tetrahydrofuran increases the strength of the mobile phase and accelerates the elution. For example, in aqueous acetonitrile amyl benzene elutes in 18 min while it elutes in only 5 min after addition of 30% tetrahydrofuran. However, a decrease in peak resolution is the penalty that must be paid for the faster separation. Thus, resolution decreases from 2.5 in aqueous acetonitrile to 1.9 and 1.1 in the mobile phase with the highest percentage of for benzene–toluene and toluene–ethylbenzene pairs, respectively (Table 6). The mobile phase containing 20% water, 60% acetonitrile, and 20% tetrahydrofuran enhances the speed while keeping sufficient resolution for baseline separation.

3.6. Effect of temperature

HPLC at higher temperature is a very powerful tool for reducing the time needed for separation. This is due to a reduction in the viscosity of the mobile phase, a decrease in the diffusion coefficients of the analytes, and changes in the strength of solute–stationary phase interactions [73]. The effect of temperature on column efficiency

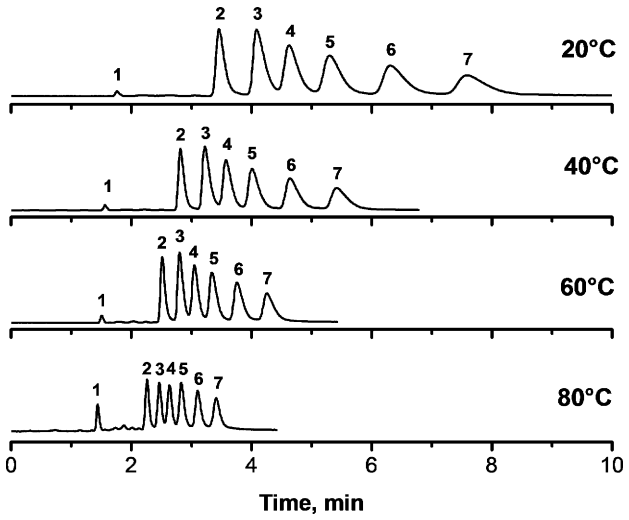

Fig. 3. Effect of temperature on the separation of small molecules using hypercrosslinked column C2. Conditions: column 100 μm × 130 mm; ternary mobile phase 20% water, 20% tetrahydrofuran, 60% acetonitrile; flow rate 0.5 μL/min; UV detection at 254 nm. Analytes: uracil (1), benzene (2), toluene (3), ethylbenzene (4), propylbenzene (5), butylbenzene (6), and pentylbenzene (7).

at isocratic separation varies case by case. Based on theoretical assumptions, an increase in temperature is expected to improve the plate counts [73]. For example, Antia and Horváth observed an improvement in efficiency while separating at elevated temperature using ODS column [74]. Similar results were described by Li and Carr for polybutadiene coated zirconia stationary phase [75]. In contrast, Vanhoenacker and Sandra demonstrated that temperature does not affect the efficiency of polydentate ODS column and only observed a shift in the minimum of the van Deemter to higher linear flow velocities [76].

Fig. 3 illustrates the considerable effect of temperature on the speed and resolution of the separation using a hypercrosslinked monolith. An increase in temperature from 20 to 80 °C reduces the run time from 8 to 3.5 min with a peak resolution exceeding 1.3 as documented in Table 7. It is worth noting that the higher temperature also positively affects peak asymmetry while peak resolution is only slightly decreased. The higher temperature also leads to a major improvement in column efficiency. The minima of van Deemter curves shown in Fig. 4 for retained benzene decrease from 28 μm at 20 °C to 16 μm at 80 °C. The latter value represents an efficiency of 60,500 plates/m. In addition, the minima are reached at higher flow velocities as a result of reduced mass transfer resistance thus enabling faster separations at higher flow rate without loss of efficiency.

The logarithm of the retention factor *vs.* reciprocal temperature plotted for all alkylbenzenes are straight lines, in which the slopes correspond to $-\Delta H/R$ where R is the gas constant, and ΔH represents the enthalpy change accompanying the transfer of the analyte from the mobile to the monolithic stationary phase. Table 8 presents the actual values of the enthalpies, which are commensurable with those found for typical reversed phase packings [75].

Table 7
Effect of column temperature on peak asymmetry of pentylbenzene AS_{PB} and resolution for peak pairs benzene–toluene $R_{BE,TO}$ and toluene–ethylbenzene $R_{TO,EB}$.

	Column temperature, °C			
	20	40	60	80
AS_{PB}	1.66	1.79	1.71	1.38
$R_{BE,TO}$	2.04	2.09	1.85	1.76
$R_{TO,EB}$	1.39	1.53	1.40	1.30

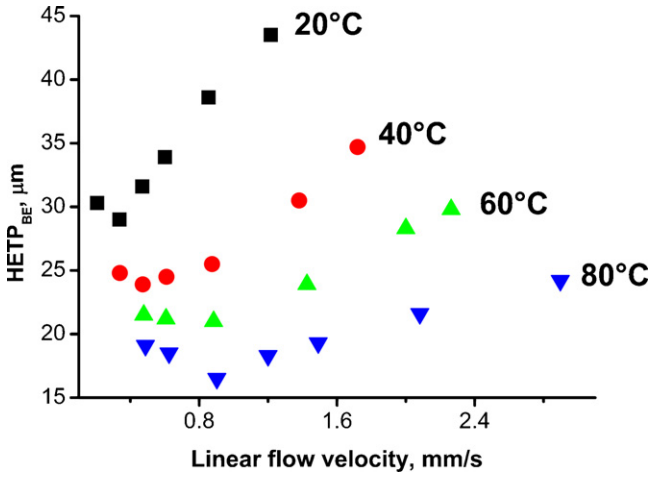

Fig. 4. Effect of temperature on van Deemter plots for benzene and hypercrosslinked monolithic column C2. Conditions: column 100 µm × 130 mm; ternary mobile phase 20% water, 20% tetrahydrofuran, and 60% acetonitrile.

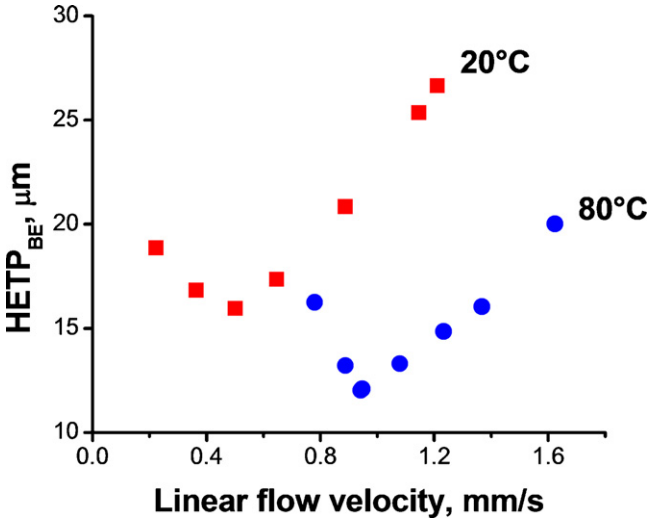

Fig. 5. Effect of temperature with very low concentration of benzene injected on van Deemter plots for benzene and hypercrosslinked monolithic column C2 at a low loading. Conditions: column 100 µm × 130 mm; ternary mobile phase 20% water, 20% tetrahydrofuran, and 60% acetonitrile; injection of benzene 0.14 pg.

Plotting the enthalpy against the number of methylene groups in the alkyl substituent affords the enthalpy change for a single methylene group that equals −0.24 kcal/mol. This value is only slightly lower than that of conventional C18 packings [75] which can be explained by the use of the ternary mobile phase since as shown in Fig. 2 tetrahydrofuran decreases the retention.

Styrene-based stationary phases are stable even at temperatures well over 200 °C. Thus, use of our hypercrosslinked columns at a temperature of 80 °C is safe. Although the mobile phase contains solvents with a boiling point lower that this temperature at standard conditions, this fact does not represent a problem in the pressurized HPLC system.

3.7. Effect of loading

Sample loading is known to exert an effect on column efficiency. Indeed, a decrease in benzene loading from 17.5 to 0.14 pg results in an increase in efficiency. Smaller loadings cannot be used due to the limit of UV detection at 3σ. The van Deemter plot in Fig. 5 obtained using injection of 0.14 pg benzene and ternary mobile phase exhibits a minimum of 16 µm at a flow velocity of 0.5 mm/s and 20 °C. This plate height corresponds to 63,200 theoretical plates/m, i.e. the value observed for separations carried out with the higher loading at 80 °C. An increase in temperature to 80 °C at the low loading enables further decrease in plate height to 12 µm that corresponds to column efficiency of 83,200 theoretical plates/m. The minimum of the plot in Fig. 5 is observed at a higher flow velocity and represents the highest column efficiency found for a column comprising organic polymer monolith used in isocratic mode.

Table 8
Enthalpy change ΔH associated with transfer of the alkylbenzenes from the ternary mobile to monolithic stationary phase calculated from slope of the logarithm of retention factor k *vs.* reciprocal temperature $1/T$ plot.

Analyte	Intercept, ln(k)	ΔH, kcal/mol	R
Benzene	−3.14	−1.81	0.99
Toluene	−3.35	−2.11	0.99
Ethylbenzene	−3.48	−2.31	0.99
Propylbenzene	−3.60	−2.51	0.99
Butylbenzene	−3.79	−2.77	0.99
Amylbenzene	−4.00	−3.04	0.99

3.8. Examples of separations

Combining the results of the optimization experiments described above enables efficient separations to be carried out at high speed. Fig. 6 demonstrates that using optimized monolith and hypercrosslinking procedure together with ternary mobile phase consisting 20% water, 20% tetrahydrofuran, and 60% acetonitrile at 80 °C, all seven compounds are separated in less than 2 min with a resolution of at least 1.0.

The hypercrosslinked column can also be used for the rapid and efficient separations of peptides. Fig. 7 shows the gradient separation of peptides of tryptic digest of cytochrome c. The separation is achieved in 10 min and the protein sequence coverage is 93.3% according to mass spectrometry.

Providing the monoliths with a multiplicity of small pores via hypercrosslinking makes them also suitable for size-exclusion chromatography. Fig. 8 presents a very good separation of four

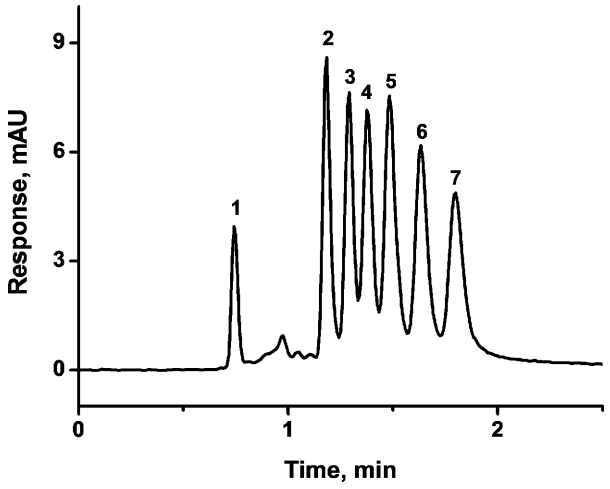

Fig. 6. Separation of small molecules at a temperature of 80 °C using the column C2 hypercrosslinked at 90 °C for 2 h and the ternary mobile phase. Conditions: column 100 µm × 130 mm; mobile phase 20% water, 20% tetrahydrofuran, and 60% acetonitrile; flow rate 1.0 µL/min; UV detection at 254 nm; back pressure 26 MPa. Analytes: uracil (1), benzene (2), toluene (3), ethylbenzene (4), propylbenzene (5), butylbenzene (6), and pentylbenzene (7).

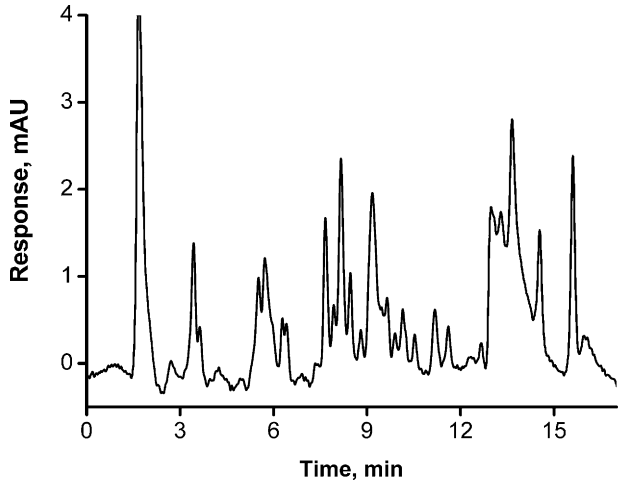

Fig. 7. Gradient elution of peptides from tryptic digest of cytochrome c using hypercrosslinked monolithic column C2. Conditions: column 100 μm × 130 mm; mobile phase A: 0.1% (v/v) formic acid in water, B: 0.1% (v/v) formic acid in acetonitrile; gradient 5–40% B in A in 10 min; flow rate 0.5 μL/min; back pressure 24 MPa; gradient delay 5 min.

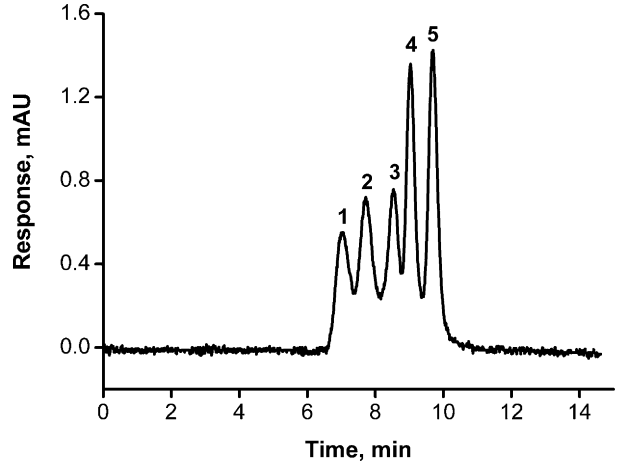

Fig. 8. Size-exclusion separation of toluene and polystyrene standards using hypercrosslinked column C2 hypercrosslinked at 80 °C for 2 h. Conditions: column 100 μm × 670 mm (320 + 350 mm); mobile phase tetrahydrofuran; flow rate 0.5 μL/min, UV detection at 254 nm; back pressure 20.5 MPa. Peaks: polystyrene with a molecular mass of 1,870,000 (1), 400,000 (2), 35,000 (3), 1000 (4), and toluene (5).

polystyrene standards and toluene using two hypercrosslinked columns C2 connected with zero-volume union. This approach was needed since our current instrumentation does not allow the preparation of columns longer than 350 mm. Despite the overall length of the column of 670 mm, the back pressure was only 20.5 MPa, i.e. within the limits easily tolerable by standard, chromatographic equipment. Our separation is the first demonstration of the use of a monolithic column in size-exclusion chromatography of polymers using an organic solvent as the mobile phase.

4. Conclusions

This report clearly demonstrates that hypercrosslinking of monolith is a powerful technique affording monolithic columns with unprecedented properties. We have illustrated the significant effects of the polymerization conditions and the post-polymerization hypercrosslinking process on the chromatographic performance of the resulting monolithic poly(styrene-*co*-vinylbenzyl chloride-*co*-divinylbenzene) stationary phase. The comprehensive optimization based on mathematical design of the composition of the polymerization mixture used to prepare the precursor monoliths, and temperature, at which the hypercrosslinking is carried out, led to an equation which facilitated the calculation of conditions that should afford columns with predetermined efficiencies. Specifically, this approach enabled the reproducible preparation of a column for (i) isocratic reversed phase separation of alkylbenzenes characterized by its high plate count, (ii) gradient elution of peptides, and (iii) very efficient size-exclusion chromatography of polystyrene standards in organic solvent. The use of high temperature and of a ternary mobile phase permits a significant acceleration of the separations. Although the hypercrosslinking approach was demonstrated with poly(styrene-*co*-vinylbenzyl chloride-*co*-divinylbenzene) monoliths, we are currently extending the hypercrosslinking process to other monoliths such as those based on functional polymethacrylates also exploring new crosslinking reactions.

Acknowledgements

Financial support of this research by a grant of the National Institute of Health (GM48364) is gratefully acknowledged. Analytical work performed at the Molecular Foundry, Lawrence Berkeley National Laboratory and F.S. were supported by the Office of Science, Office of Basic Energy Sciences, U.S. Department of Energy, under Contract No. DE-AC02-05CH11231.

References

[1] S. Hjérten, J.L. Liao, R. Zhang, J. Chromatogr. 473 (1989) 273.
[2] T.B. Tennikova, F. Svec, B.G. Belenkii, J. Liquid Chromatogr. 13 (1990) 63.
[3] F. Svec, J.M.J. Fréchet, Anal. Chem. 54 (1992) 820.
[4] H. Minakuchi, K. Nakanishi, N. Soga, N. Ishizuka, N. Tanaka, Anal. Chem. 68 (1996) 3498.
[5] A.I. Liapis, J.J. Meyers, O.K. Crosser, J. Chromatogr. A 865 (1999) 13.
[6] E. Riccardi, J.C. Wang, A.I. Liapis, J. Chromatogr. Sci. 47 (2009) 459.
[7] G. Guiochon, J. Chromatogr. A 1168 (2007) 101.
[8] P. Gzil, G.V. Baron, G. Desmet, J. Chromatogr. A 991 (2003) 169.
[9] P. Gzil, N. Vervoort, G.V. Baron, G. Desmet, J. Sep. Sci. 27 (2004) 887.
[10] F. Svec, J.M.J. Fréchet, Science 273 (1996) 205.
[11] D. Josic, A. Buchacher, A. Jungbauer, J. Chromatogr. B 752 (2001) 191.
[12] M.R. Buchmeiser, Macromol. Rapid Commun. 22 (2001) 1082.
[13] F. Svec, T.B. Tennikova, Z. Deyl, Monolithic Materials: Preparation, Properties, and Applications, Elsevier, Amsterdam, 2003.
[14] F. Svec, J. Sep. Sci. 27 (2004) 1419.
[15] A. Jungbauer, R. Hahn, J. Sep. Sci. 27 (2004) 767.
[16] F. Svec, C.G. Huber, Anal. Chem. 78 (2006) 2100.
[17] J. Urban, P. Jandera, J. Sep. Sci. 31 (2008) 2521.
[18] M.R. Buchmeiser, Polymer 48 (2007) 2187.
[19] N.W. Smith, Z. Jiang, J. Chromatogr. A 1184 (2008) 416.
[20] E.G. Vlakh, T.B. Tennikova, J. Chromatogr. A 1216 (2009) 2637.
[21] A. Nordborg, E.F. Hilder, Anal. Bioanal. Chem. 394 (2009) 71.
[22] R. Bakry, C.W. Huck, G.K. Bonn, J. Chromatogr. Sci. 47 (2009) 418.
[23] Q. Wang, F. Svec, J.M.J. Fréchet, Anal. Chem. 65 (1993) 2243.
[24] A. Premstaller, H. Oberacher, C.G. Huber, Anal. Chem. 72 (2000) 4386.
[25] M. Petro, F. Svec, I. Gitsov, J.M.J. Fréchet, Anal. Chem. 68 (1996) 315.
[26] Q. Wang, F. Svec, J.M.J. Fréchet, J. Chromatogr. A 669 (1994) 230.
[27] P. Coufal, M. Cihak, J. Suchankova, E. Tesarova, Z. Bosakova, K. Stulik, J. Chromatogr. A 946 (2002) 99.
[28] D. Moravcova, P. Jandera, J. Urban, J. Planeta, J. Sep. Sci. 26 (2003) 1005.
[29] D. Moravcova, P. Jandera, J. Urban, J. Planeta, J. Sep. Sci. 27 (2004) 789.
[30] Y. Huo, P.J. Schoenmakers, W.T. Kok, J. Chromatogr. A 1175 (2007) 81.
[31] H. Aoki, T. Kubo, T. Ikegami, N. Tanaka, K. Hosoya, D. Tokuda, N. Ishizuka, J. Chromatogr. A 1119 (2006) 66.
[32] Z. Xu, L. Yang, Q. Wang, J. Chromatogr. A 1216 (2009) 3098.
[33] Y. Li, D.H. Tolley, M.L. Lee, J. Chromatogr. A 1217 (2010) 4934.
[34] S.H. Lubbad, M.R. Buchmeiser, J. Sep. Sci. 32 (2009) 2521.
[35] S.H. Lubbad, M.R. Buchmeiser, J. Chromatogr. A 1217 (2010) 3223.
[36] L. Trojer, C.P. Bisjak, W. Wieder, G.K. Bonn, J. Chromatogr. A 1216 (2009) 6303.
[37] A. Greiderer, L. Trojer, C.W. Huck, G.K. Bonn, J. Chromatogr. A 1216 (2009) 7747.
[38] I. Nischang, O. Bruggemann, J. Chromatogr. A 1211 (2010).
[39] E.C. Peters, F. Svec, J.M.J. Fréchet, C. Viklund, K. Irgum, Macromolecules 32 (1999) 6377.
[40] C. Viklund, K. Irgum, F. Svec, J.M.J. Fréchet, Macromolecules 34 (2001) 4361.
[41] U. Meyer, F. Svec, J.M.J. Fréchet, C.J. Hawker, K. Irgum, Macromolecules 33 (2000) 7769.
[42] V.A. Davankov, S.V. Rogozhin, M.P. Tsyurupa, US 538 Pat 3,729,457 (1971).

[43] A.V. Pastukhov, M.P. Tsyurupa, V.A. Davankov, J. Polym. Sci., Polym. Phys. 37 (1999) 2324.
[44] V.A. Davankov, M.P. Tsyurupa, React. Polym. 13 (1990) 27.
[45] V.A. Davankov, M. Tsyurupa, M. Ilyin, L. Pavlova, J. Chromatogr. A 965 (2002) 65.
[46] M.P. Tsyurupa, V.A. Davankov, React. Funct. Polym. 66 (2006) 768.
[47] P. Veverka, K. Jerabek, React. Funct. Polym. 59 (2004) 71.
[48] J.H. Ahn, J.E. Jang, C.G. Oh, S.K. Ihm, J. Cortez, D.C. Sherrington, Macromolecules 39 (2006) 627.
[49] C.D. Wood, B. Tan, A. Trewin, H. Niu, D. Bradshaw, M.J. Rosseinsky, Y.Z. Khimyak, N.L. Campbell, R. Kirk, E. Stockel, A.I. Cooper, Chem. Mater. 19 (2007) 2034.
[50] J.Y. Lee, C.D. Wood, D. Bradshaw, M.J. Rosseinsky, A.I. Cooper, Chem. Commun. (2006) 2670.
[51] J. Germain, J. Hradil, F. Svec, J.M.J. Fréchet, Chem. Mater. 18 (2006) 4430.
[52] J. Germain, J.M.J. Fréchet, F. Svec, Polym. Mater., Sci. Eng. 97 (2007) 272.
[53] V.A. Davankov, C.S. Sychov, M.M. Ilyin, K.O. Sochilina, J. Chromatogr. A 987 (2003) 67.
[54] C.S. Sychov, M.M. Ilyin, V.A. Davankov, K.O. Sochilina, J. Chromatogr. A 1030 (2004) 17.
[55] N.A. Penner, P.N. Nesterenko, M.M. Ilyin, M.P. Tsyurupa, V.A. Davankov, Chromatographia 50 (1999) 611.
[56] J. Urban, F. Svec, J.M.J. Fréchet, Anal. Chem. 82 (2010) 1621.
[57] U.D. Neue, HPLC Columns: Theory, Technology, and Practice, Wiley, New York, 1997.
[58] H. Engelhardt, High-pressure Liquid Chromatography, 1977.
[59] J. Seidl, J. Malinsky, K. Dusek, W. Heitz, Adv. Polym. Sci. 5 (1967) 113.
[60] K. Jerabek, Anal. Chem. 57 (1985) 1598.
[61] K. Jerabek, K. Setinek, J. Hradil, F. Svec, React. Polym. 5 (1987) 151.
[62] H. Aoki, N. Tanaka, T. Kubo, K. Hosoya, J. Polym. Sci., Polym. Chem. 46 (2008) 4651.
[63] S. Lubbad, M.R. Buchmeiser, Macromol. Rapid Commun. 23 (2002) 617.
[64] B.P. Santora, M.R. Gagne, K.G. Moloy, N.S. Radu, Macromolecules 34 (2001) 658.
[65] W. Wieder, S.H. Lubbad, L. Trojer, C.P. Bisjak, G.K. Bonn, J. Chromatogr. A 1191 (2008) 253.
[66] K. Cabrera, D. Lubda, H.M. Eggenweiler, H. Minakuchi, K. Nakanishi, HRC J. 23 (2000) 93.
[67] J. Urban, S. Eeltink, P. Jandera, P.J. Schoenmakers, J. Chromatogr. A 1182 (2008) 161.
[68] L. Geiser, S. Eeltink, F. Svec, J.M.J. Frechet, J. Chromatogr. A 1140 (2007) 140.
[69] J. Urban, D. Moravcova, P. Jandera, J. Sep. Sci. 29 (2006) 1064.
[70] J. Urban, P. Jandera, P.J. Schoenmakers, J. Chromatogr. A 1150 (2007) 279.
[71] B. Ells, Y. Wang, F.F. Cantwell, J. Chromatogr. A 835 (1999) 3.
[72] L.D. Bowers, S. Pedigo, J. Chromatogr. 371 (1986) 243.
[73] T. Teutenberg, Anal. Chim. Acta 643 (2009) 1.
[74] D. Antia, C. Horváth, J. Chromatogr. 435 (1988) 1.
[75] J. Li, P.W. Carr, Anal. Chem. 69 (1997) 837.
[76] G. Vanhoenacker, P. Sandra, J. Sep. Sci. 29 (2006) 1822.